

Ulysses Observations of Alfvén Waves in the Southern and Northern Solar Hemispheres

E.J. Smith

Jet Propulsion Laboratory, California Institute of Technology, Pasadena, California

A. Balogh

Imperial College of Science and Technology, The Blackett Laboratory, London, England

M. Neugebauer

Jet Propulsion Laboratory, California Institute of Technology, Pasadena, California

D. McComas

Los Alamos National Laboratory, Los Alamos, New Mexico

Abstract

Alfvén waves with periods from < 1 to > 10 hours are continuously present in the sun's south and north polar regions. The recent fast latitude scan of Ulysses resulted in an abrupt decrease in wave power below $\approx 30^\circ$ latitude. The correlations between magnetic field and solar wind velocity fluctuations, upon which the wave identification is based, indicate outward propagation in both hemispheres. The waves are linearly polarized in that the field and velocity fluctuations are in-phase although without a preferred plane of polarization. The long period waves propagate radially rather than along the average field, a discrepancy compared to in-ecliptic observations which is explained. Because of the long wavelengths, which reach ≈ 0.3 AU, the waves are resonant with 10 - 10^3 MeV/nucleon galactic cosmic rays and oppose their entry into the polar caps. The wave amplitudes imply a contribution to the acceleration of the high latitude wind due to momentum transfer of

only a few percent. The possible influence of the waves on long duration terrestrial aurorae is discussed.

Introduction

As Ulysses passed above 45° south heliographic latitude, hourly variances in the three components of the magnetic field along the radial, R, tangential or azimuthal, T, and meridional or north-south, N, directions showed a persistent increase [Smith et al., 1995]. The corresponding variances in the field magnitude changed only slightly. Analysis of the waveforms evident in both the field vector, \vec{B} , and solar wind velocity, \vec{V} , showed that they were highly correlated implying that the major contributor to the fluctuations was Alfvén waves which were propagating away from the sun.

Observations as the spacecraft traveled to the highest latitude (-80.2°) and returned to the solar equator have revealed the continuous presence at high latitude of these large amplitude, long period waves [Balogh et al., 1995a]. Continuous measurements over this and the subsequent interval have been analyzed to determine the characteristic properties of the waves and to investigate their changes with latitude and radial distance. Many of the most important findings are presented here.

The Alfvén waves are undoubtedly a characteristic feature of the high speed solar wind issuing from the polar coronal holes and may be influencing its origin and acceleration [Belcher, 1971; Alazraki and Couturier, 1971]. Alfvén waves seen intermittently in the solar equatorial region [Belcher et al., 1969; Denskat et al., 1981] are probably related to those at high latitude. The presence of the waves throughout the polar cap has significant implications for the accessibility of galactic cosmic rays to the high latitude heliosphere [Jokipii and Kota, 1989]. The waves may originate from a basic wave-particle instability such as the firehose instability [Parker, 1963] and/or be a consequence of the random

motion of the ends of the field lines in the photosphere [Jokipii and Parker, 1968]. These issues are commented on briefly from the perspective of the Ulysses observations.

Observations and Analysis

The basic correlation between fluctuations in the field, $\delta\vec{B}$, and in the solar wind velocity, $\delta\vec{V}$, is graphically illustrated in figure 1. The hourly averages of the transverse components (V_N, B_N are shown) are especially well correlated. Correlograms of this kind have been prepared and analyzed for many intervals of approximately one solar rotation (or 26 days). The analysis of Belcher and Davis [1971] was used which refrains from treating either of the parameters as an independent variable and the other as a dependent variable. This procedure is equivalent to obtaining the least squares straight line from the ratio of the standard deviations of, e.g., δV_N and δB_N . For the example shown, the slope, $\delta V/\delta B=24\text{km/s}\cdot\text{nT}$, and the correlation coefficient is 0.72.

The sign of the slope, or of the correlation coefficient, is always positive as in figure 1. When combined with the inward-directed sense of the average magnetic field in the southern hemisphere, the Alfvén relation between δV and δB implies that the waves are outwardly-propagating. This sense of propagation is a characteristic feature of the waves throughout the high latitude region. The waves are also linearly polarized as expected from the Alfvén relation, i.e., there is no significant phase shift between δV and δB , although the plane of polarization is random.

It is evident from figure 1 that the Alfvén waves include periods, T , significantly longer than an hour. A variant of the correlation coefficient that contains information about the periods is the correlation function or its Fourier transform expressed as the coherency [Bendat and Piersol, 1971]. Figure 2 shows the amplitude and phase of the coherency

between δB_N and δV_N for the data contained in figure 1. Frequency, f , is shown along the bottom and period, T , along the top scale.

The magnitude (solid line) is large, exceeding a value of 0.7 for ' t ' \leq 10 hours. The phase relation between δB_N and δV_N , given by the dashed line, shows that the two parameters are in phase, i.e., the waves are propagating outward at all these periods. By contrast, similar analysis carried out by Belcher and Davis [1971] revealed a cutoff of the in-ecliptic Alfvén waves at a period of ≈ 2.5 hours, q'bus, the high latitude waves exhibit significantly longer periods.

Another important wave property is their direction of propagation. A variance analysis of the field variations has been carried out for examples like figure 1. Typically, the two largest eigenvalues are about equal and much larger than the smallest eigenvalue. The eigenvector corresponding to the latter is nearly aligned with the radial direction, the other two eigenvectors being transverse to \hat{R} . This result implies that the average wave normal, corresponding to the direction of propagation, is nearly radial, as predicted by theory. However, the Alfvén waves studied in the ecliptic using the same general approach indicated that the waves were propagating along the average field direction. This inconsistency has been a problem for many years.

An alternative approach which shows graphically that the high latitude waves are propagating radially is to consider the associated electric field variations. The electric fields in the spacecraft frame have been computed from $E = -V \times \vec{B}$. The results for the same interval as in figure 1 are shown in figure 3. The three components of E in the radial, azimuthal and meridional directions are shown along with the resultant magnitude. Clearly, the electric field variations are principally transverse ($E_N, E_T \gg E_R$), implying propagation along the radial direction.

The correlations between the field and velocity have also been used to study changes in wave amplitude with time. The correlation coefficients of the hourly values of the three components have been determined over successive solar rotations [Bendat and Piersol, 1971]. This approach enables long time intervals to be studied as in figure 4 where 3.5 years are represented. The heliographic latitude of Ulysses is shown along the upper scale.

Before the boundary of high speed coronal hole flow was reached, the correlation coefficients, $\rho(B,V)$, show large variations about zero. A gradual increase beginning in 1993.5 coincides with entry into the high speed flow as seen in the solar wind measurements at this time. The dominant feature in the figure is the long interval in which $\rho(B_T, V_T)$, $\rho(B_N, V_N)$ are large (≥ 0.7) and steady which implies the continuous presence of Alfvén waves at high latitude.

Another significant feature is the abrupt drop in the correlations as Ulysses returned northward to the equator and passed into the north hemisphere. The increasing speed of the spacecraft as it approached perihelion produced a rapid traversal of latitudes from -80.2° to 0° to $40^\circ N$ which resulted in a sudden disappearance of the waves. This decrease occurred at a latitude of $\approx 30^\circ S$, roughly the latitude at which the waves were seen when the spacecraft was traveling poleward. After passage of the equatorial zone, the correlation coefficients once again became large but with a reversed sign. This reversal was expected because the field is now directed outward in the north hemisphere. The negative correlation shows that the waves are propagating outward in the north hemisphere also.

The availability of continuous measurements during the long interval of over a year allows power spectra to be computed that extend to very low frequencies or very long periods. The power spectra of the B_T component and the magnitude are shown in figure 5

with the periods shown along the upper scale. The $/B/$ spectrum has a slope of approximately $-5/3$ at the highest frequencies. The component spectrum has a slope of approximately -1 over much of the frequency range until becoming flat at very low frequencies ($T \approx 10$ days). Although these spectra are revealing, they are taken over a significant range of radial distances and further analysis will be required to infer how different frequency bands vary with distance and/or latitude.

Discussion

There are two important observational differences between the Alfvén waves reported here and those that have been detected for many years in the ecliptic, first near 1 AU by Mariner 5 and then nearer the sun by Helios. The high latitude waves extend to much longer periods, 10-20 hours as compared to 2 to 3 hours at low latitude. This difference may simply be the result of the intermittent nature of the low latitude wind. High latitude, high speed wind is seen at low latitude because of the tilt of the Heliospheric Current Sheet (HCS) and associated structures and is normally present for only a few hours to about one day before corotating back to higher latitudes. Thus, the waves may not be present long enough to reveal the longest periods. Although this explanation is plausible, there are other possibilities such as a difference in the wave periods in the interior of the polar coronal hole and at its low latitude boundary. In any case, the existence of the long period waves has important consequences as discussed below.

The other important difference concerns the directions of propagation, radial at high latitude but field-aligned at low latitude. The latter conclusion is based on the variance analysis carried out by Belcher and Davis [1971]. In retrospect, a significant consideration is that their analysis extended to only $T \leq 22.5$ minutes, i.e., the shorter periods. Our analysis discussed above was based on much longer periods. The two results are not as

inconsistent as they may appear at first, The shorter period waves probably propagate along and are guided by the longer period, longer wavelength waves in a manner analogous to the waves seen on the surface of a lake or ocean. The long period water waves propagate parallel to the surface on average while the short period waves follow the local variations in the surface. Successive variance analyses carried out for the short period fluctuations show that they are following the average field direction as anticipated [T. Horbury, private communication].

The longest wavelengths of the high latitude waves are a substantial fraction of an AU. The Alfvén speed is still only a small fraction of the solar wind speed of ≈ 750 km/sec so that the waves are basically being convected. Using the above speed, waves with a period of 10 hours have a wavelength: $\lambda = (750) (3.6 \times 10^4) = 2.7 \times 10^7$ km = 0.18 AU. For a period of 1 hour, the wavelength is 0.018 AU.

These wavelengths are comparable to the gyro radii of galactic cosmic rays. For cosmic rays having energies of 1 GeV/nucleon, the gyro radius in a 1 nT field (representative of the field at Ulysses) is $p = 0.0377$ AU. The resonant wavelength, given by $\lambda = 2\pi p$, is 0.237 AU. For energies of 100 and 10 MeV/nucleon, the corresponding resonant wavelengths are 0.063 and 0.019 AU. Thus, the Alfvén waves would be expected to strongly influence the galactic cosmic rays and, in particular, should inhibit their access to the polar heliosphere. The modest increase in the intensity of the galactic cosmic rays at high latitudes observed by the Ulysses experiments is generally attributable to this cause [Simpson et al., 1995].

The very long wavelengths suggest that the field variations may be those predicted by Jokipii and Kota [1989] following an earlier proposal that convective motions in the photosphere would produce a random walk of the field lines threading the surface [Jokipii

and Parker, 1968], It was argued that the motions would be communicated outward along the field lines “adiabatically”, i.e., their amplitude would decrease as r^{-1} instead of $r^{-3/2}$ as predicted by the WKB approximation for Alfvén waves propagating away from the sun in the solar wind. In companion articles, it is shown that the field variances follow an r^{-3} dependence at the shorter periods [Balogh et al., 1995b] but transition toward r^{-2} at longer periods as predicted [Jokipii et al., 1995].

The shorter wavelength waves may not all originate at the sun. One possibility with a long history is that they may result from a firehose instability. Such waves are generated when the plasma flow becomes highly anisotropic and the pressure parallel to the field, p_{\parallel} , exceeds the sum of the perpendicular pressure, p_{\perp} , and the tension in the curved field lines. Thus, the condition for instability can be expressed as

$$p_{\parallel} > p_{\perp} + B^2/4\pi \text{ or as } A^2 = 1 - 4\pi(p_{\parallel} - p_{\perp})/B^2 < 1.$$

Calculations using the observed pressure anisotropies in the solar wind in the presence of the Alfvén waves yield a typical value of $A \approx 0.7$ [Goldstein et al., 1995]. Although this result implies that the firehose instability is not operating, locally, conditions for wave growth may hold nearer the sun. Furthermore, the pickup of freshly ionized interstellar neutrals may increase the pressure asymmetry and excite the firehose instability [Goldstein et al., 1995]. The evolution of the waves with distance is complex, involving non-linear effects characteristic of turbulence, and will require careful study.

The discovery of the outward-propagating Alfvén waves in the ecliptic led to the suggestion that the momentum of the solar wind came, in part, from the equivalent pressure gradient introduced by the waves [Belcher, 1971; Alazraki and Couturier, 1971]. The effect of the Alfvén waves on the acceleration of the solar wind can be assessed by comparing the energy flux density of the waves at the sun, $S_W = \frac{\langle \delta B_s^2 \rangle}{4\pi} v_s$, extrapolated to 1 AU, with the measured energy flux density of the solar wind, $S_K = \frac{1}{2} \rho v^3$.

In the above equations, $\langle \delta B^2 \rangle$ is the mean square value of the fluctuations in the field, $V_{Ar} = Br/(4\pi\rho)^{1/2}$ is the radial Alfvén speed and p and V are the solar wind density and velocity. Equipartition of wave magnetic and kinetic energies is assumed. Subscript S refers to the sun.

The wave amplitudes at the sun and 1 AU are related by an invariant, I , obtained from the solution of the solar wind flow equations, including wave pressure, in the WKB (short wavelength) limit [Hollweg, 1974]:

$$I = (1 + V_{Ar})^2 (V/V_{Ar})^2 \langle \delta B^2 \rangle.$$

The ratio of the two flux densities expressed in terms of measurements at 1 AU is given by Roberts [1989]:

$$\frac{S_w}{S_K} = \frac{2 \langle \delta B^2 \rangle}{B_r^2} \left(\frac{V_{Ar}}{V} \right) \left(1 + \frac{V_{Ar}}{V_{ASW}} \right)^2$$

For the Ulysses observations at high latitude, a typical value of $\langle \delta B^2 \rangle / B_r^2 = 0.3$. The solar wind speed is $\approx 750 \text{ km s}^{-1}$ and the Alfvén speed (reduced by a factor of 0.7 to allow for a pressure anisotropy with $p_{\parallel} > p_{\perp}$ [Goldstein et al., 1995]) is only $V_{Ar} = 20 \text{ km s}^{-1}$. Thus, $\frac{S_w}{S_K} = 2(0.3)(20/750)(1 + 20/750)^2 = 0.017 \approx 1/60$.

This ratio is approximately ten times smaller than the conservative value of $\approx 1/6$ obtained by Roberts [1989] using $\langle \delta B^2 \rangle / B_r^2 \approx 1.0$ and $V_{Ar}/V \approx 0.07$. It shows that in the high speed, high latitude solar wind, the momentum transfer from the waves to the wind is small, contributing only a few percent to the solar wind flux density. This conclusion cannot be avoided by appealing to the effect of longer period waves since numerical calculations by Heineman and Olbert [1980] show that most of the transfer is accounted for by the waves included in the WKB approximation.

An interesting implication of the high latitude waves is their effect on the terrestrial magnetosphere. Not only does the high speed of the solar wind correlate with geomagnetic activity generally, but the Alfvén waves that are then present for long intervals give rise to intense, long duration aurorae [Tsurutani et al., 1990]. The physical explanation that has been advanced involves quasi-periodic reconnection of the varying heliospheric field and the terrestrial magnetic field. Thus, a plausible connection is established between the earth and high latitude regions of the sun.

Acknowledgments

Joyce Wolf participated in the analysis and prepared the figures, J. Hollweg assisted in evaluating the wave contribution to solar wind acceleration. Discussions with R.J. Jokipii, M.L. Goldstein and M. Lee are greatly appreciated. The results presented here represent one aspect of research done by JPL-CIT under contract to NASA. Financial Support to ICST was provided by the U.K. Particle Physics and Astronomy Research Council.

•

References

- Alazraki, G. and P. Couturier, Solar wind acceleration caused by the gradient of Alfvén wave pressure, *Astron. & Astrophys.*, 13, 380-389, 1971.
- Balogh, A., E.J. Smith, B.T. Tsurutani, D. Southwood, R.J. Forsyth, T.S. Horbury, The heliospheric magnetic field over the south polar region on the sun, *Science*, 268, 1007-1010, 1995a.
- Balogh, A., R.J. Forsyth, T.S. Horbury, E. Smith, Variances of the large scale fluctuations in the heliospheric magnetic field out of the ecliptic plane, *Geophys. Res. Lett.*, Submitted 1995b.
- Belcher, J. W., L. Davis, Jr., and E.J. Smith, Large-amplitude waves in the interplanetary medium: Mariner 5, *J. Geophys. Res.*, 74, 2302-2308, 1969.
- Belcher, J.W., L. Davis, Jr., Large-amplitude Alfvén waves in the interplanetary medium, *J. Geophys. Res.*, 76, 3534-3563, 1971,
- Belcher, J. W., Alfvénic wave pressures and the solar wind, *Astrophys. Journal*, 168, 509-524, 1971,
- Bendat, J. S., and A.G. Piersol, *Random Data: Analysis and Measurement Procedures*, Wiley -Interscience, New York, 1971.
- Denskat, K. U., F.M. Neubauer and R. Schwenn, Properties of "Alfvénic" fluctuations near the sun: Helios-1 and Helios-2, in *Solar Wind Four*, Ed. H. Rosenbauer, Report MPAE-W-100-81-3I, p. 392-397, 1981.
- Goldstein, B. E., M. Neugebauer and E.J. Smith, Alfvén waves, alpha particles and pickup ions in the solar wind, to appear in *Geophys. Res. Lett.*, 1995,
- Heinemann, M. and S. Olbert, Non-WKB Alfvén waves in the solar wind, *J. Geophys. Res.*, 85, 1311-1327, 1980.
- Hollweg, J.V. Transverse Alfvén waves in the solar wind: Arbitrary $v_0 B_0$ and $|\delta B|$, *J. Geophys. Res.*, 79, 1539-1541, 1974,
- Jokipii, J. R., and E.N. Parker, Random walk of magnetic lines of force in astrophysics, *Physical Review Letters*, 21, 44-47, 1968.
- Jokipii, J. R., and J. Kota, The polar heliospheric magnetic field, *Geophys. Res. Lett.*, 16, 1-4, 1989.
- Jokipii, J. R., J. Kota, E.J. Smith, T.S. Horbury, A. Balogh, and J. Giacalone, Large scale magnetic variances observed at high heliographic latitude: Interpretation, radial variation and cosmic ray effects, *Geophys. Res. Lett.*, Submitted 1995.
- Parker, E.N. *Interplanetary Dynamical Processes*, John Wiley & Sons, New York, p.154, 1963.

Roberts, D. A., Interplanetary observational constraints on Alfvén wave acceleration of the solar wind, *J. Geophys. Res.*, 94, 6899-6905, 1989.

Simpson, J. A., J.D. Anglin, V. Bothmer, J.J. Connell, P. Ferrando, B. Heber, H. Kunow, C. Lopate, R.G. Marsden, R.B. McKibben et al., Cosmic ray and solar particle investigations over the south polar regions of the sun, *Science*, 268, 1019-1023, 1995.

Smith, E. J., M. Neugebauer, B. Tsurutani, Ulysses observations of latitude gradients in the heliospheric magnetic field: Radial component and variances, *Space Science Reviews*, 72, 165-170, 1995.

Tsurutani, B. T., T. Gould, B.E. Goldstein, W.D. Gonzalez, M. Sugiura, Interplanetary Alfvén waves and auroral (substorm) activity: IMP-8, *J. Geophys. Res.*, 95, 2241, 1990.

Figure Captions

Fig.1 Correlogram of V_N vs B_N

Corresponding hourly averages of the northward component of solar wind velocity and magnetic field (in RTN or Solar Heliospheric, SH, coordinates) are shown. The interval covered is 30 days in mid-1994 when Ulysses was in the south polar cap approaching maximum latitude. The straight line fit is derived without assuming B_N is the independent variable as in the usual formulas for a least squares fit (see Belcher and Davis 1971).

Fig. 2 Coherency of V_N, B_N

The coherency defined, for example, in Bendat and Piersol [1971] is shown as a function of frequency or period (upper scale) for the same interval as in figure 1. The amplitude (solid line) shows a continuously high correlation ≈ 0.75 at all periods from 2 to ≈ 20 hours. The phase (dashed line) shows that V_N and B_N are in-phase throughout the same extended interval.

Fig. 3 Electric Field Components and Magnitude Observed at High Latitude

The four parameters computed from $\vec{E} = -\vec{V} \times \vec{B}$ are shown. The components are in solar heliospheric (RTN) coordinates as before. The interval covered is the same 30 days as in figures 1 and 2. The striking feature is the electric fields associated with the Alfvén waves in E_T and E_N and the absence of a significant component in E_R consistent with radial propagation. The units, $nT \cdot km \cdot s^{-1}$, are equivalent to $1 \mu v \cdot m^{-1}$. The average value of E_N is negative corresponding to the electric field associated with the Parker Spiral.

Fig, 4 Correlation Coefficients of V_N-B_N and V_T-B_T : 1992-1995

The correlation coefficients normalized to unity [Bendat and Piersol, 1971] are plotted over successive 26 day intervals from post-Jupiter encounter (1992) through the fast latitude scan (see upper scale) and passage of Ulysses into the north hemisphere. Large correlations from $50^\circ S$ to $30^\circ S$ and above $30^\circ N$ are caused by the continuous presence of the Alfvén waves in the absence of significant solar wind structure. The sign reversal in 1995 is caused by the change to an outward-directed magnetic field.

Fig. 5 Power Spectra of High Latitude Fluctuations

The continual presence of the Alfvén waves at high latitude over the extended interval shown allows the power spectra to cover very low frequencies or long periods of 2 hours to > 10 days (top scale). There is significantly more power in B_N than in B_{\perp} as expected. Dashed straight lines with slopes of $f^{-5/3}$ and f^{-1} are shown. For periods of 2 to 24 hours, the observed spectra are consistent with f^{-1} , both spectra becoming flatter at longer periods. The spectra are convolved with an as yet undetermined function of radial distance. The variances show that different frequencies obey different radial dependence.

Ulysses, 1994, Days 182-212

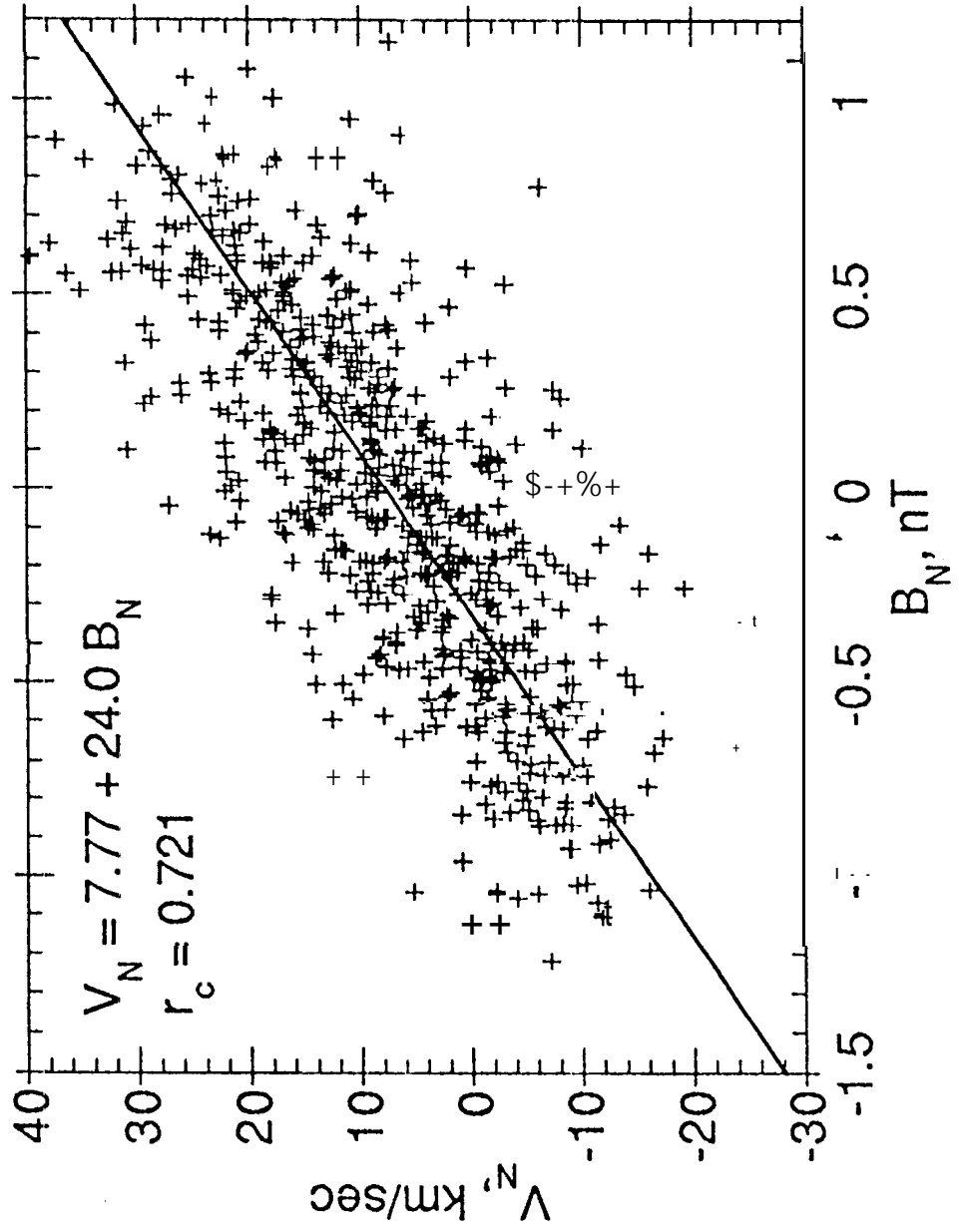


Figure 1

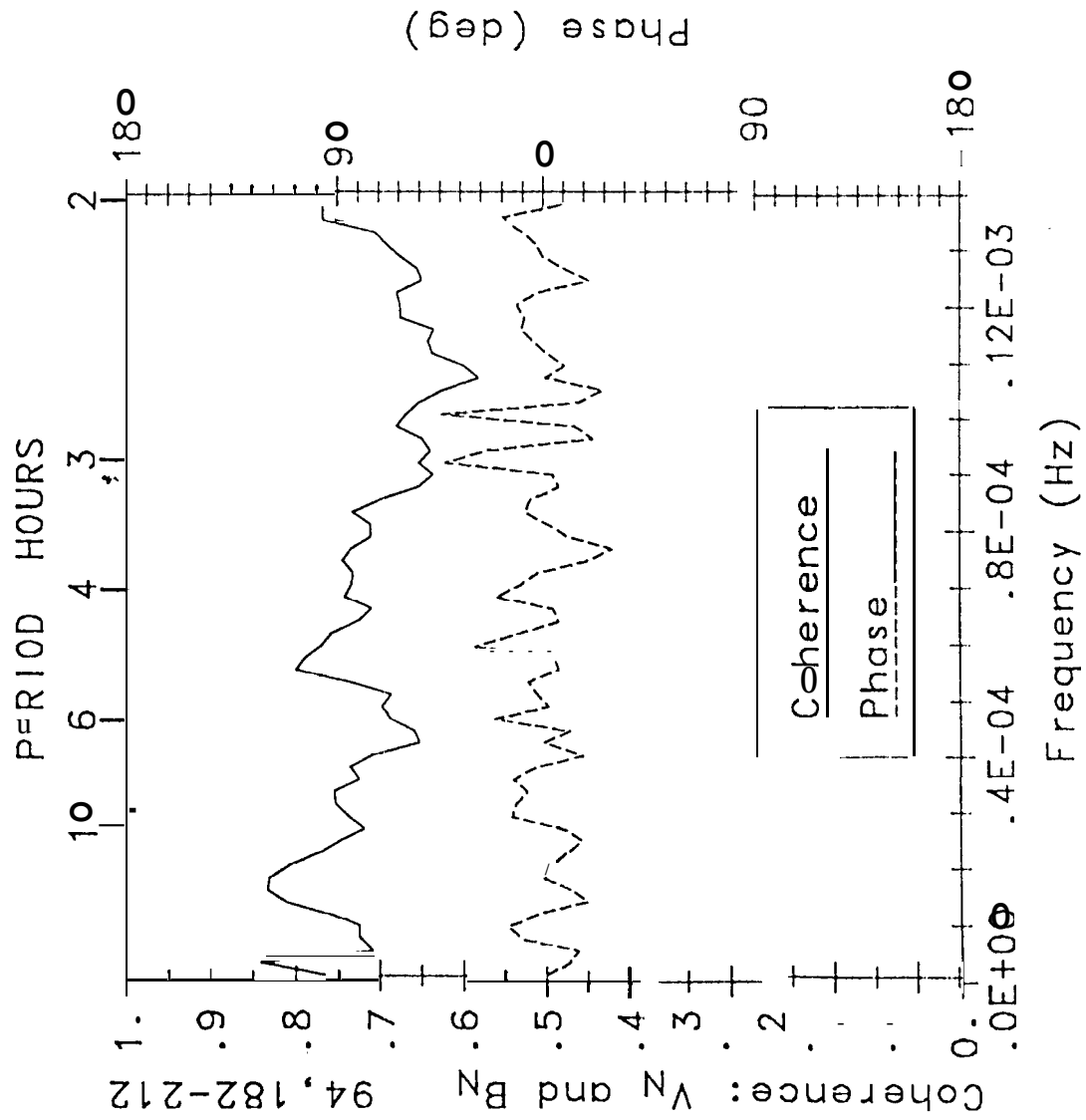
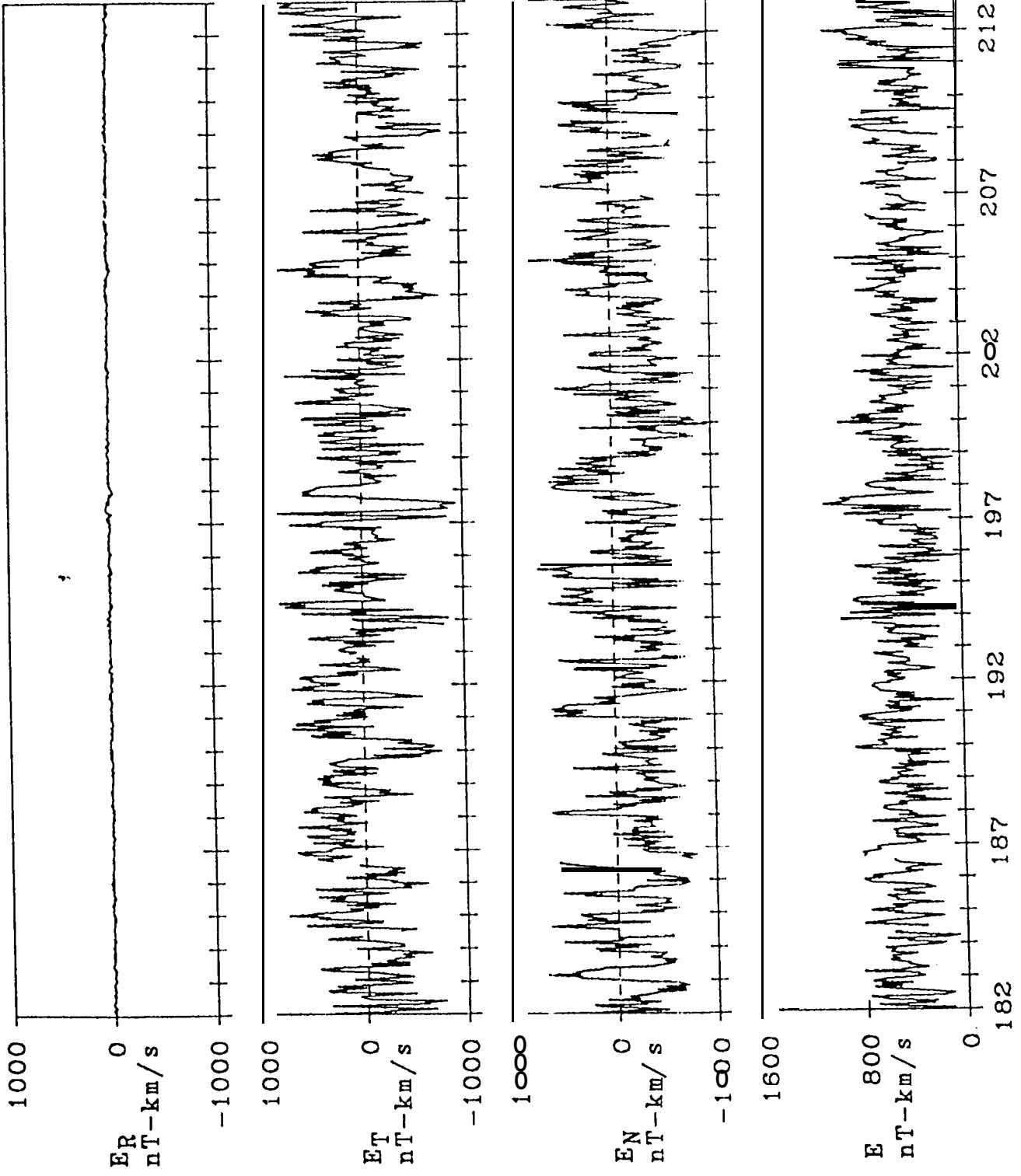


Figure 2

ELECTRIC FIELDS

Jul 1 - Jul 31, 1994 (182-212)



DAY OF YEAR 1994

Figure 3

Correlations for 26-day periods of Ulysses hour averages

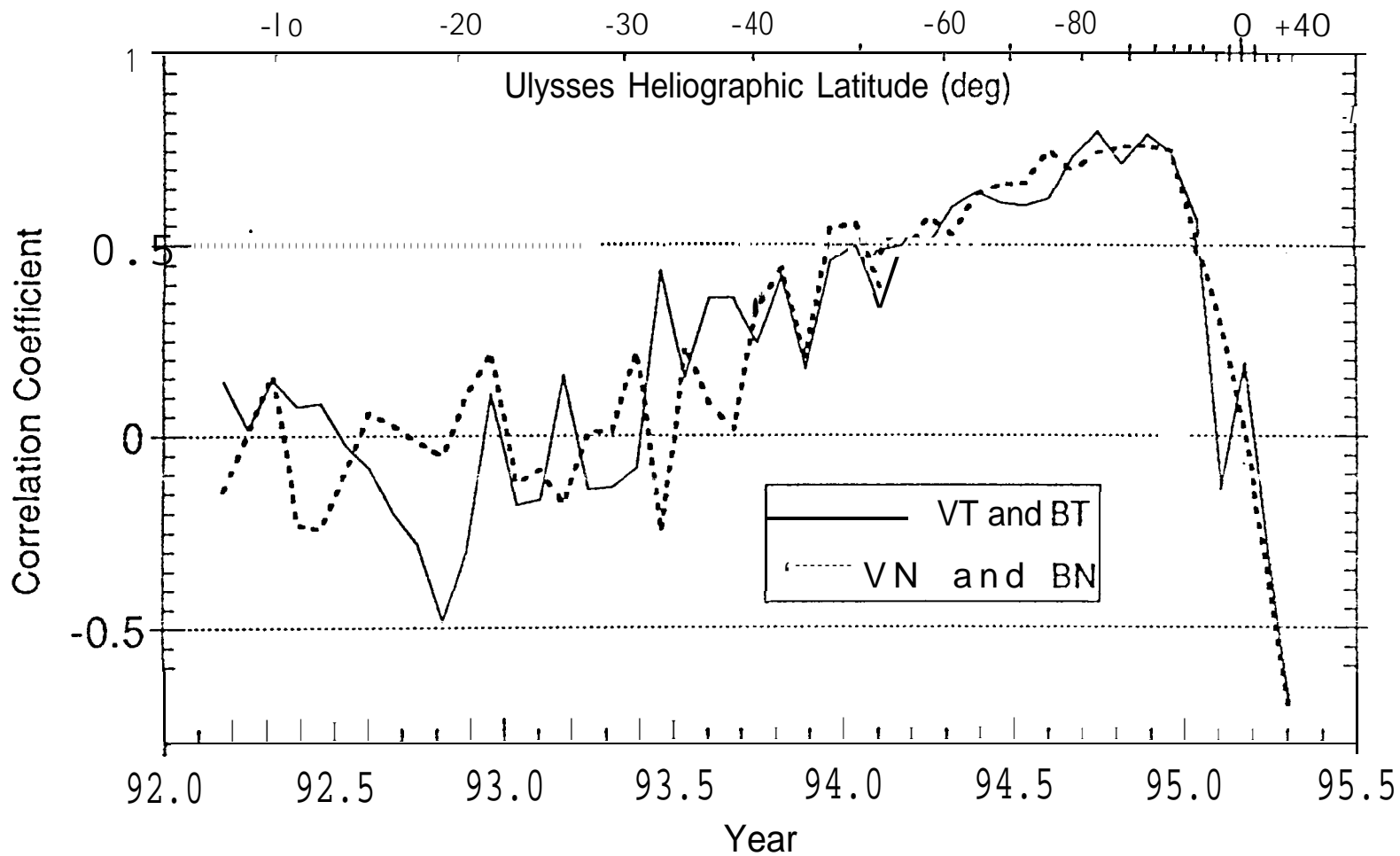


Figure 4

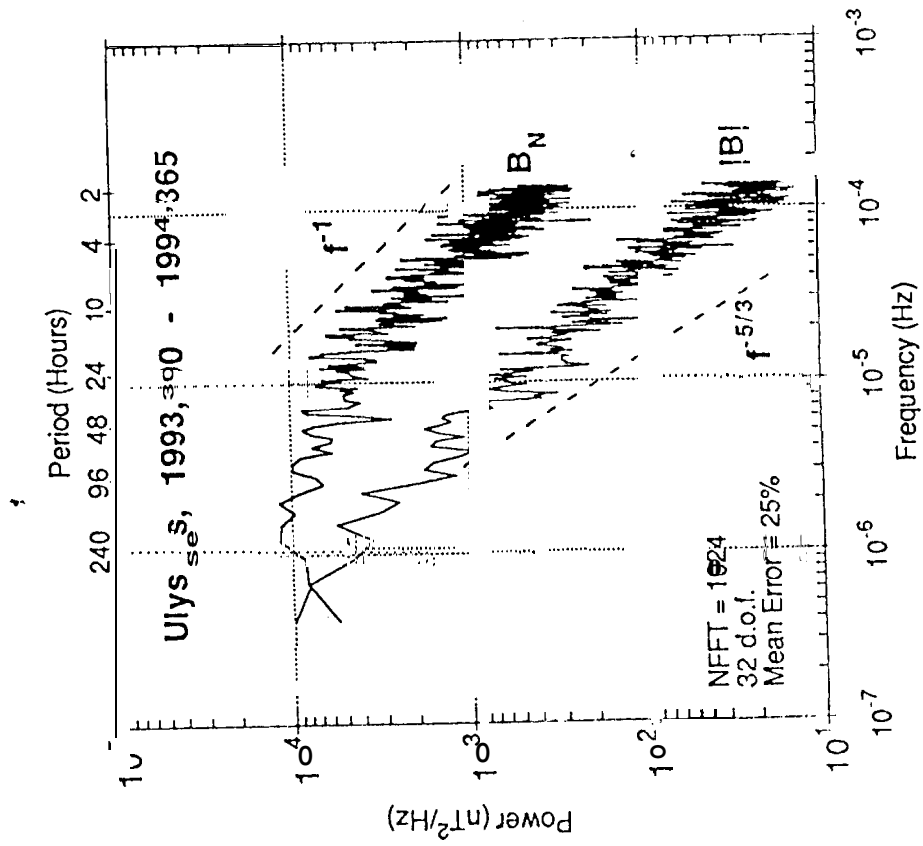


Figure 5